The Astrophysical Journal, 954:91 (7pp), 2023 September 1 https://doi.org/10.3847/1538-4357/ace975

Lithium in Turnoff Stars in the Globular Cluster M5: A Quest for Primordial Lithium

Ann Merchant Boesgaard[1,3] and Constantine P. Deliyannis[2,3]
[1] Institute for Astronomy, University of Hawai'i at Manoa, 2680 Woodlawn Drive, Honolulu, HI 96822, USA; annmb@hawaii.edu, boes@ifa.hawaii.edu
[2] Department of Astronomy, Indiana University, 727 East 3rd Street, Swain Hall West 319, Bloomington, IN 47405-7105, USA; cdeliyan@indiana.edu
Received 2023 June 27; revised 2023 July 19; accepted 2023 July 19; published 2023 August 25

Abstract

The light element lithium is formed by nucleosynthesis during the Big Bang. Its abundance can help to define the parameters of the early Universe. To find this primordial value, it is necessary to determine Li abundances in the oldest stars because it is readily destroyed by nuclear reactions in stellar interiors. We have made high-resolution (∼45,000) spectroscopic observations of five identical unevolved turnoff stars in the 13 Gyr old globular cluster M5. In our analysis we find a range in Li abundance of a factor of 2; the spread is 5 times the individual error. The comparison of these results with those for turnoff stars from five other globular clusters reveals a similarly large range in Li. Lithium in M5 and the other clusters all have stars above the field star Li plateau, but none are as high as the predictions for primordial Li. The maximum values for Li are the same in all six clusters. Multiple generations of stars are found in many globular clusters; those later generations are expected to have formed from Li-depleted gas. Such second- and later-generation stars would have no Li. However, only one of the six clusters has a few unevolved stars with upper limits on the Li abundance.

Unified Astronomy Thesaurus concepts: Stellar abundances (1577); Stellar atmospheres (1584); Stellar astronomy (1583); Stellar interiors (1606)

1. Introduction

The study of the element Li has provided information on nucleosynthesis during the Big Bang. Along with ^{2}H, ^{3}He, and ^{4}He, ^{7}Li is produced during the first 15 minutes of the Universe by neutrons and protons. However, Li is easily destroyed in stars and can also be created in the interstellar medium through spallation by energetic (150 MeV) particle collisions with abundant C, N, O atoms. To establish the value of the primordial Li it is necessary to to measure it in the oldest, unevolved stars in the Galaxy. The earliest attempt at this was the study of Li in the most metal-poor field stars by Spite & Spite (1982). A recent example extends Li abundances down to a star having [Fe/H] = −6.1 (Aguado et al. 2019). Other very metal-poor stars in the galactic halo, both dwarfs and giants, have been studied for Li and other elements by Bandyopadhyay et al. (2022).

The unevolved stars in the oldest globular clusters provide another venue for establishing the primordial value of Li. One of the oldest and most metal-poor globular clusters is M92. In a compilation of 68 globular clusters by age, Valcin et al. (2020) give 13.30 ± 0.06 Gyr for M92. Recently, Ying et al. (2023) determine the absolute age of M92 to be 13.80 ± 0.75. Bailin (2019) tabulates the metallicities for 55 globular clusters and gives $[Fe/H] = -2.239 \pm 0.028$ for M92. We reported on the Li abundances in several turnoff stars in M92 (Deliyannis et al. 1995; Boesgaard et al. 1998). We found a range in Li abundance of a factor of 3 in our five stars with similar temperatures, all near 5800–5900 K. The spread in $A(\mathrm{Li}) = \log N(\mathrm{Li}) - \log N(\mathrm{H}) + 12.00$ was 2.01 to 2.45, which was attributed to differences in initial angular momenta and then spindown. The slowest rotators would lose the least Li while the rapid rotators would undergo more Li depletion via mixing to hotter interior regions where Li would be destroyed by reactions with protons.

Large studies of Li in globular clusters that include turnoff stars have been done for four southern globular clusters. Aoki et al. (2021) studied 357 stars from the turnoff to red giants in 47 Tuc. Lind et al. (2009) observed Li in 349 stars in NGC 6397 of which 180 were turnoff stars, while Gonzalez Hernandez et al. (2009) found Li abundances in 163 stars in that cluster. NGC 6752 was studied for Li by Shen et al. (2010) in 112 turnoff stars. Both Monaco et al. (2012) and Spite et al. (2016) examined Li abundances in 91 main-sequence and subgiant stars in M4.

Unevolved stars in globular clusters contain information about the basic composition of the stars before they have undergone any mixing with their internal layers during post-main-sequence evolution. One important caveat to this idea is that multiple generations of star formation have occurred as discussed in a review by Gratton et al. (2012). Their Figure 6 shows examples of the well-known Na–O anticorrelation in 20 globular clusters. Early generations of massive stars that explode into supernovae in star-forming regions will enrich that next generations. This could result in a spread in metallicity even in the first population of stars. Lardo et al. (2023) found evidence for this in NGC 2808.

Here we are studying Li in the main-sequence turnoff stars in M5 for the first time with high-resolution spectra. These stars have $V = 18$, some 2–6 magnitudes fainter than the red giants. There is excellent CCD photometry of M5 by Sandquist et al. (1996). They find an age for M5 of 13.5 ± 1 Gyr with [Fe/H] = −1.40 (Zinn & West (1984) and 11 ± 1 Gyr with [Fe/H] = −1.17 (Sneden et al. (1992). The most quoted value of [Fe/H] is −1.33 from Carretta et al. (2009) and is between those two. Although M5 is an old globular cluster (12.75 ± 0.08 Gyr; Valcin et al. 2020), it has a metallicity at the median for the 19

[3] Visiting Astronomer, W. M. Keck Observatory, jointly operated by the California Institute for Technology and the University of California.

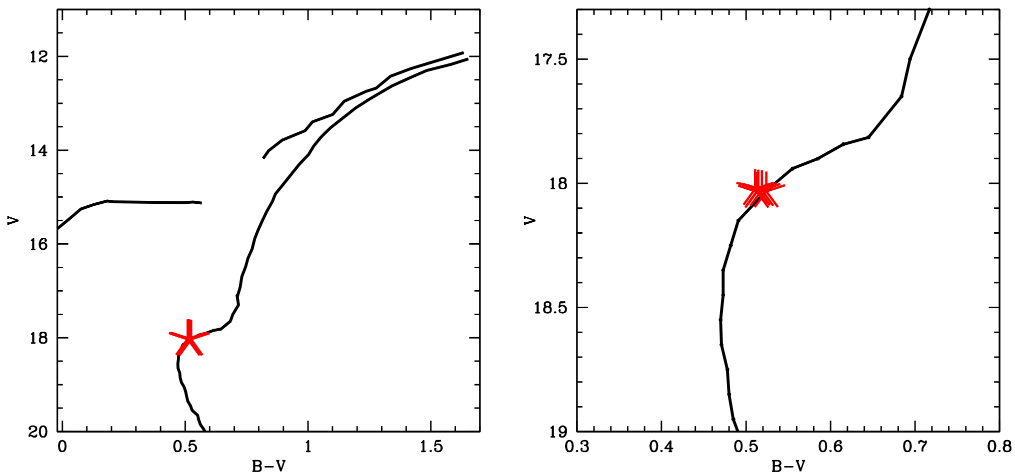

Figure 1. Color–magnitude diagram for M5 from Sandquist et al. (1996). Left: the full diagram showing their best fit to the observations. The stars we observed are shown as red stars. Right: an enlargement of the main-sequence and turnoff sections of their color–magnitude diagram with our stars as red stars. Note the faintness of our five stars and their similarity.

Table 1
Log of the Keck/HIRES Observations of M5 Stars

Star	V	σ	$B-V$	σ	(Date-UT)	Exp (minutes)	Total (minutes)	S/N
5287	18.0224	0.0036	0.5108	0.0074	1999 May 10	5 × 45		
					1999 May 11	1 × 45	270	39
5303	18.0243	0.0043	0.5145	0.0074	1999 May 10	3 × 50		
						1 × 45	195	38
5323	18.0270	0.0036	0.5187	0.0073	1999 May 11	6 × 45	270	37
5351	18.0319	0.0036	0.5240	0.0080	1999 Jun 08	1 × 45		
						5 × 60	345	35
5364	18.0338	0.0036	0.5128	0.0058	1999 Jun 07	2 × 45		
						4 × 60	330	32

clusters compiled by Carretta et al. (2009) and is given a value for [Fe/H] $= -1.259 \pm 0.003$ in the collection of Bailin (2019).

A special feature of this research is that the five stars are virtually identical in V, $(B-V)_0$, $T_{\rm eff}$, and log g.

Lithium abundances in M5 have been reported for 99 red giant stars by D'Orazi et al. (2014) with spectral resolution of 17,000. They find values for A(Li) predominantly between 0.8 and 1.1. This represents the dilution of Li in red giants caused by the expansion of the surface convection zone.

2. Observations and Stellar Parameters

The turnoff stars in M5 have $V = 18.0$, but it was possible to observe them at high spectral resolution with HIRES (Vogt et al. (1994) on the Keck I telescope. Figure 1 shows the fit through the data for the color–magnitude diagram for M5 from Sandquist et al. (1996). The positions of the nearly identical five stars we observed are shown by red stars at $V = 18.0$.

Multiple exposures were required to obtain high enough signal-to-noise ratios (S/Ns), but with a limit of 45–60 minutes on each exposure. The exposure times had to be long enough to obtain good signal, but not so long that they were subjected to too many cosmic-ray events. On each night there were at least two exposures of the Th–Ar lamp, one at the beginning of the night and one at the end. We took 15–20 quartz flat-field frames and 15–20 bias frames.

The log of our spectral observations of five turnoff stars in M5 appears in Table 1. The photometry is from Sandquist et al. (1996). The total observing time for each star of the coadded spectra is between 195 and 345 minutes. The echelle spectra have 29 orders and cover from 4425 to 6880 Å with some interorder gaps at longer wavelengths. The spectral resolution is ~45,000 or ~0.04 Å pix^{-1} in the Li I region. The data reduction was done with IRAF (Tody 1986, 1993)[4] including bias subtraction, flattening, and wavelength calibration from the Th–Ar reference lamp. The individual spectra for each star were wavelength adjusted, then coadded. Those coadded spectra were then fit with a continuum with IRAF.

We show the Li region of the coadded, continuum-fit wavelength corrected spectra for two of the stars in Figure 2. These spectra have comparable S/Ns. The temperatures of the two stars agree with each other within 25 K. The positions of the Li I and Ca I lines are indicated. While the Ca I line strengths are seen to be similar in the two stars, the Li I line is clearly stronger in 5323 than in 5351.

We have measured equivalent widths of several Fe I lines in those same two stars, 5323 and 5351, and show those results in Figure 3. The 45° line shows where the measurements would be equal for the two stars. The median difference is 5.4 mÅ for each pair of lines. The difference for the Li I line in the two stars is 19.9 mÅ.

In our past work on Li abundances in globular clusters we have used temperatures scales derived by Carney (1983)

[4] IRAF is distributed by the National Optical Astronomy Observatories, which are operated by The Association of Universities for Research in Astronomy, Inc. now NOIRLab, under cooperative agreement with the National Science Foundation.

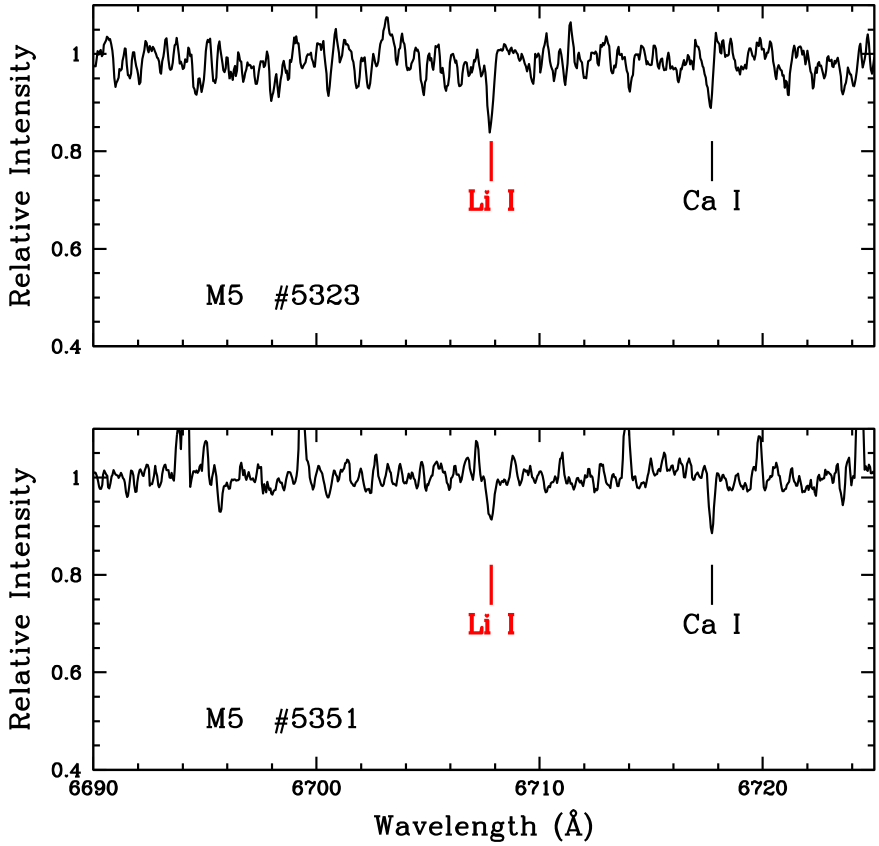

Figure 2. Examples of spectra of two stars in the Li region. The positions of the Li I and Ca I features are indicated. The Ca I lines are similar in strength in both stars, while the Li I feature is stronger in 5323.

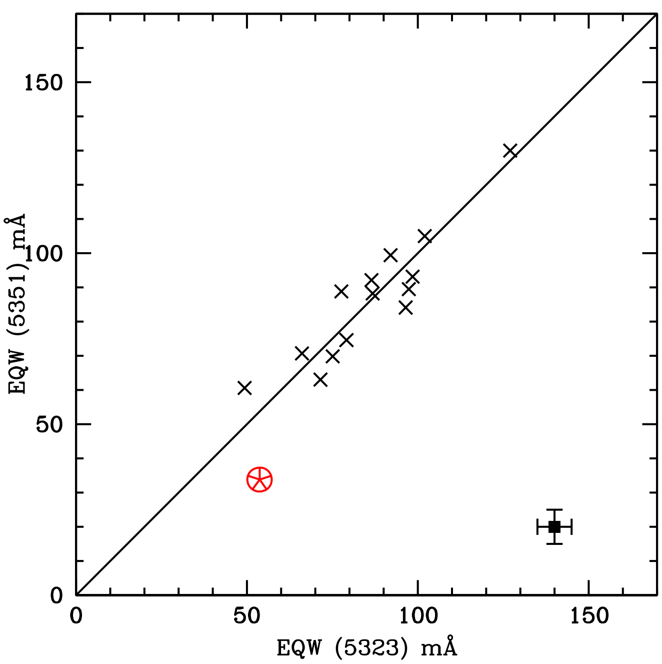

Figure 3. The equivalent width measurements for two stars in M5. The crosses are for several Fe I lines and the red-circled star is for the Li I line, which is stronger in the star 5323. The line indicates equality in the equivalent widths. An error bar for the line strength measurements is shown in the lower right and corresponds to ±5 mÅ.

and King (1993) from $(B-V)$ colors. We now include a temperature scale from Ramirez & Melendez (2005) based on the infrared flux method (IRFM). The King scale results in the hottest temperatures and the Ramirez & Melendez the coolest with a difference of ∼210 K. Each of our five stars are close to each other in temperature on any of the scales. For a given temperature scale our five stars differ by less than 60 K and less than 0.05 in log *g*. We can conclude that they are quintuplets.

3. Lithium Abundances

We have determined Li abundances with the spectrum analysis program MOOG[5] (Sneden 1973; Sneden et al. 2012). We used the stellar parameters in Table 2 on all three temperature scales. Abundances of Li were found by spectrum synthesis with *synth*.

Examples of the synthesis fits for two stars are shown in Figure 4, from the Carney (1983) temperature scale. The best-fit syntheses show that these two stars differ in Li by a factor of 1.8. Our line list includes the Li doublet and hyperfine structure. It also includes a line of Fe I at 6707.441 that contributes virtually nothing at these temperatures. We also found the Li abundances with the *blends* feature in MOOG from the measured equivalents widths.

The results are given in Table 3 for all five stars with all three temperature scales for both the synthetic spectrum results and the equivalent with measurements. We prefer the results from the spectrum synthesis, but note the agreement between the two techniques is very good with a mean difference of 0.05 in *A*(Li).

The Li abundances are sensitive to temperature, but not to the other model parameters. A change of +60 K results in a

5 https://www.as.utexas.edu/~chris/moog.html

Table 2
Stellar Parameters

Star	$T_{\rm eff}$ (K)	log g
M5:5287	C83 5906	3.92
	K93 6039	4.00
	RM05 5830	3.84
M5:5303	C83 5890	3.91
	K93 6024	3.95
	RM05 5815	3.87
M5:5323	C83 5871	3.90
	K93 6007	3.98
	RM05 5798	3.82
M5:5351	C83 5848	3.89
	K93 5986	3.97
	RM05 5775	3.81
M5:5364	C83 5897	3.92
	K93 6031	4.00
	RM05 5822	3.84

change in A(Li) of +0.04 dex. The two stars shown in Figure 4 differ in $T_{\rm eff}$ by 58 K and in A(Li) by 0.25 dex or 6 times greater than errors due to temperature.

It is of interest to examine further whether the apparent differences in A(Li) between these stars are real, as opposed to simply reflecting errors. We proceed in a manner similar to that in our M92 work.

The stars were deliberately chosen to have near-identical temperatures, so that differences in A(Li) would simply be a reflection of differences in the equivalent width of the Li line. We then apply the Cayrel (1988) formulation for calculating errors in equivalent widths, as recast by Deliyannis et al. (1995). The 1σ error due to photon noise alone, $\sigma_{\rm ph}$, depends on the width of the line and the S/N per pixel. We assume that the 1σ error due to continuum placement, $\sigma_{\rm co}$, is of similar magnitude and then add that in quadrature to $\sigma_{\rm ph}$ to get the total a total 1σ error, $\sigma_{\rm tot}$. As a check of these procedures and assumptions, we measured 14 Fe I lines on the linear part of the curve of growth in stars 5323 and 5351 (see Figure 3) and found an average difference of 6.54 mA, or 4.62 mÅ per measure. The average width of these lines is 137 mÅ (with a dispersion of 47 mÅ per pixel), and the S/N per pixel is nearly identical for both stars, 37 and 35, respectively. This yields $\sigma_{\rm ph}$ = 3.35 mÅ and $\sigma_{\rm tot}$ = 4.73 mÅ, nearly identical to the value 4.62 mÅ indicated above.

The width of the Li I doublet is 185 mÅ, a bit larger than that for the Fe I lines, as expected, and thus yields slightly larger errors for these stars of $\sigma_{\rm ph}$ = 3.89 mÅ and $\sigma_{\rm tot}$ = 5.50 mÅ. The measured Li equivalent widths are 53.7 and 33.8 mÅ, respectively, which are solid detections at the 9.8σ and 6.1σ levels, respectively; their difference is 19.9 mÅ. A chi-squared test suggests that there is only a 0.00030 probability of obtaining the measured equivalent widths purely by chance with the given errors (and assumptions) if the real equivalent widths are identical.

We repeat this analysis for stars 5287 and 5364, which have an even smaller difference in temperature (about 8 K) than stars 5323 and 5351 (about 23 K). But the difference in S/N per pixel is larger: 39 and 32, respectively. Once again, the measured Li equivalent widths are strong detections at the 10.5 and 5.3σ levels, respectively. For simplicity, we adopt S/N = 32 for both stars, which may overestimate the error for star 5287. Then, a chi-squared test suggests that there is only a 0.00094 (or smaller) probability of obtaining the measured equivalent widths purely by chance with the given errors if the real equivalent widths are identical.

Whether we compare star 5323 to 5351, or star 5287 to 5364, there is strong evidence that there is a real dispersion in A(Li) in our M5 sample.

For our M5 stars the corrections for effects of non-LTE and 3D on Li line formation are small. Wang et al. (2021) calculated these effects on three Li I lines including the resonance line, λ6707 of our observations. Their results, as highlighted in their Figure 8, indicate corrections of less than −0.04 in A(Li) for our range in $T_{\rm eff}$, log g, and [Fe/H].

4. Discussion

Both Figure 4 and Table 3 show that there is a range in Li abundances in our five otherwise-identical stars. The spread is a factor of 2. All but one of the stars has a Li amount greater than the field star plateau of A(Li) = 2.2. These results are similar to our findings for Li in six turnoff stars in M92 (Boesgaard et al. 1998) with a range in A(Li) of 0.44 dex and half of them above the field star plateau.

Abundances of Li have been determined in other globular clusters. NGC 6397 was studied for Li first by Pasquini & Molaro (1996) in six stars with three near the turnoff. Later Bonifacio et al. (2002) determined Li abundances of 12 turnoff stars. There were 79 main-sequence stars included in the research by Gonzalez Hernandez et al. (2009). In addition, Koch et al. (2011) reported a turnoff star that is super Li-rich with A(Li) = 4.03.

For NGC 6752 there were nine turnoff stars in the Li study by Pasquini et al. (2005). Schiappacasse-Ulloa et al. (2022) found Li abundances in 217 stars, of which 156 were turnoff and subgiant branch stars. Their range for Li in the turnoff stars was A(Li) = 2.4 down to an upper limit of 1.6. Gruyters et al. (2014) looked into the effects of atomic diffusion on Li (and several other elements) in 194 stars from the turnoff to red giants. For the turnoffs they found A(Li) values from 2.1 to 2.4 with three stars with only upper limits on Li. Shen et al. (2010) found a correlation between Li and O in a sample of 112 turnoff stars and suggest that there would be Li production in the polluting gas.

The abundance of Li has been determined in 91 stars in the globular cluster M4 by Monaco et al. (2012) and Spite et al. (2016). Of those stars there are 52 with temperatures above 5800 K and log g larger than 4.00. They show a range in A(Li) from 1.82 to 2.40. They comment on one star in this range that has a "remarkably" large Li value at 2.87 and discuss possibilities for this at some length.

One of the most metal-rich globular clusters is 47 Tuc = NGC 104. Pasquini & Molaro (1997) found Li abundances in two turnoff stars, and Bonifacio et al. (2007) determined Li with high-resolution spectra of four turnoff stars. A major work on Li was done by Aoki et al. (2021). They found Li abundances for 93 turnoff stars in their total sample of 347 stars. Their range in A(Li) was 1.5–2.3 for the turnoff stars.

A compilation of the ages of globular cluster has been done by Valcin et al. (2020) and of [Fe/H] values by Bailin (2019). We show these values for the six clusters in Table 4. (Note that the Planck collaboration age of the Universe is 13.7 Gyr, while the age given by Valcin et al. is 14.21 Gyr.) The results for A(Li) in turnoff stars are shown in Figure 5 as a function of the cluster Fe abundance. Of the six clusters M5 is the youngest at

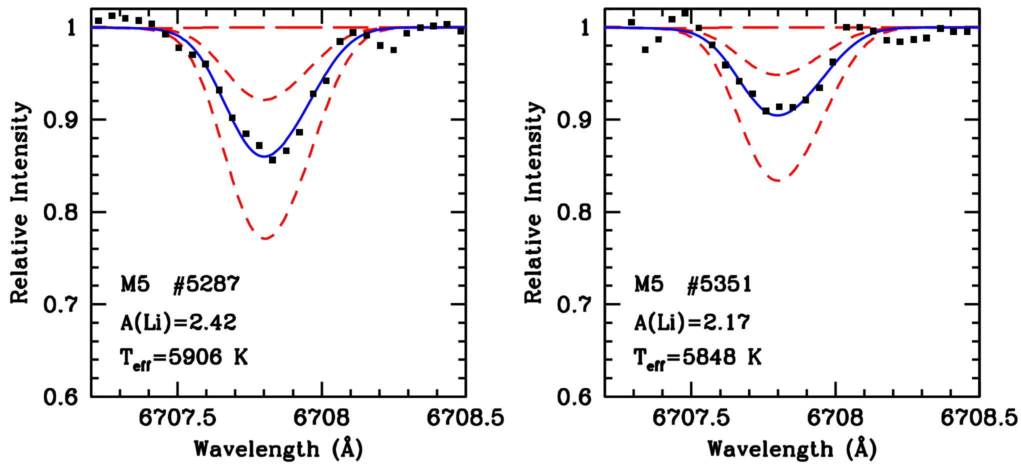

Figure 4. The spectrum synthesis fits for Li in two of our stars. The black squares are the observed spectra, and the blue solid line is the best fit. The red dashed lines are a factor of 2 more Li and a factor of 2 less Li; the long-dashed red line represents no Li at all. The temperatures and A(Li) values are for the Carney (1983) temperature scale.

Table 3
Lithium Abundances

Star	T(K)	T(C)	T(R)	$A(\mathrm{Li})_K$	$A(\mathrm{Li})_C$	$A(\mathrm{Li})_R$	EQW	$A(\mathrm{Li})_K$	$A(\mathrm{Li})_C$	$A(\mathrm{Li})_R$
5287	6039	5906	5830	2.53	2.42	2.37	53.3	2.57	2.47	2.41
5303	6024	5890	5815	2.55	2.45	2.45	47.9	2.51	2.40	2.33
5323	6007	5871	5798	2.48	2.35	2.35	53.7	2.55	2.45	2.38
5351	5986	5848	5775	2.30	2.17	2.10	33.8	2.30	2.18	2.13
5364	6031	5897	5822	2.38	2.28	2.24	32.8	2.32	2.21	2.14
RANGE	53	58	55	0.25	0.28	0.35	20.9	0.27	0.29	0.28

12.75 Gyr, but cluster age does not seem to affect the measured Li abundance or the spread in Li in turnoff stars.

We see these indications from Figure 5:

(1) All six clusters show a large range in A(Li) in these unevolved stars.

(2) All have many stars above the field star Li plateau.

(3) All of these unevolved stars have Li detections; except for a few stars in NGC 6752, none have upper limit values for A(Li).

(4) None has an amount of Li that is near the predictions for primordial Li.

(5) The maximum A(Li) abundance for all six clusters is similar, near 2.5 dex.

The explanation for the values and the range in A(Li) values that we proposed for M92 (Boesgaard et al. 1998) was that differences in initial angular momentum played an important role in the preservation, or lack thereof, of the surface content of Li. The most rapid rotators would spin down the most and destroy the most Li. The slower rotators would not spin down as much and so preserve more Li. All the stars may have lost some of their initial Li from a potentially higher initial amount.

This "rotational mixing" could account for the spread in the Li content. The two stars with the lowest A(Li) (stars 5351 and 5364) have lower A(Li) ($\sim$2.22) than the two stars 5287 and 5303) with the highest A(Li) ($\sim$2.43). It could also account for the result that the Li abundances of all our stars lie below the value $A(\mathrm{Li}) = 2.7$–2.8 inferred from Planck data in the context of standard Big Bang nucleosynthesis.

The formalism of how models with a variety of rotational instabilities should be constructed was pioneered by Endal & Sofia (1976) and Endal & Sofia (1981). The Yale-style models predict that such depletion may vary slightly from star to star because of differences in the initial stellar angular momenta (e.g., Pinsonneault et al. 1989, 1992; Somers & Pinsonneault 2016).

Table 4
Globular Cluster Ages and Metallicities

NGC	Name	Age (Gyr)	[Fe/H]
NGC 104	47 Tuc	13.54 ± 0.90	-0.747 ± 0.003
NGC 5904	M5	12.75 ± 0.80	-1.259 ± 0.003
NGC 6121	M4	13.01 ± 1.01	-1.166 ± 0.004
NGC 6341	M92	13.30 ± 0.60	-2.239 ± 0.028
NGC 6397	⋯	14.21 ± 0.69	-1.994 ± 0.004
NGC 6752	⋯	13.47 ± 0.67	-1.583 ± 0.003

This rotational mixing has explained many observations in Populations I dwarfs about the surface depletion of Li, Be, and B. For example, higher than normal Li abundances were observed in short-period tidally locked binaries (Thorburn et al. 1993; Ryan & Deliyannis 1995); the cool side of the "Li Dip" discovered by Boesgaard & Tripicco (1986) and the correlated depletion of Li and Be (Deliyannis et al. 1998; Boesgaard et al. 2004) and of Be and B in F dwarfs (Boesgaard et al. 2005, 2016); the Li–temperate relation and the Li/Be ratio of M67 subgiants evolving out of the cool side of the Li Dip (Sills & Deliyannis 2000; Boesgaard et al. 2020); the correlation between stellar spindown and Li depletion in late A/early F dwarfs (Deliyannis et al. 2019); and the continued depletion of Li during the main sequence in G dwarfs (Boesgaard et al. 2022, Sun et al. 2023). Explanation of Li abundances in late

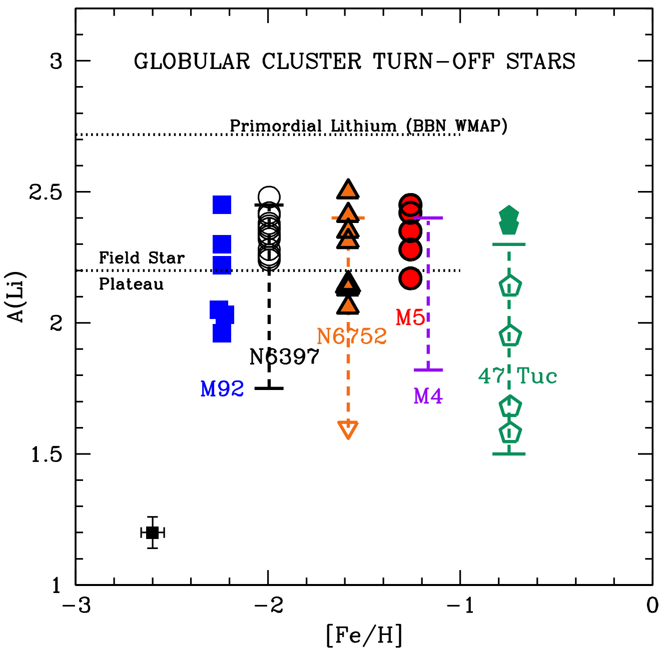

Figure 5. Lithium abundances in turnoff stars in several globular clusters with a range of iron abundances. The results for M5 are from this work, on the Carney temperature scale, shown as filled red circles. The results for M92 from Boesgaard et al. (1998), also on the Carney temperature scale, are shown as blue filled squares; two stars with identical Li values are offset from each other for clarity. The values for NGC 6397 are from Bonifacio et al. (2002) and Pasquini & Molaro (1996), shown as open black circles. The range in values for NGC 6397, shown by the vertical black dashed line, are from Lind et al. (2009) and Gonzalez Hernandez et al. (2009). The orange triangles for NGC 6752 represent nine stars from Pasquini et al. (2005). The range for 217 turnoff stars, shown as the vertical dashed line, is from Gruyters et al. (2014) and Schiappacasse-Ulloa et al. (2022). There are 52 turnoff stars in M4 shown as a range in A(Li) as the purple dashed vertical line from Monaco et al. (2012) and Spite et al. (2016). The values for 47 Tuc (NGC 104) are from Pasquini & Molaro (1997), shown as green filled pentagons, and those by Bonifacio et al. (2007) by open green pentagons. The green dashed line shows the range of values for turnoff stars for 47 Tuc found by Aoki et al. (2021). A typical error bar is shown in the lower left corner. The horizontal line at A(Li) = 2.2 represents the mean abundance of Li found for metal-poor field stars first identified by Spite & Spite (1982). The horizontal line at A(Li) = 2.719 corresponds to the predicted value for primordial Li indicated by the WMAP results (Cyburt et al. 2008 and Cyburt et al. (2016).

G/K dwarfs may in addition require magnetically induced radius inflation (Somers & Pinsonneault 2015; Jeffries et al. 2021).

Conclusion (3) above is more difficult to explain. When high-mass, first-generation stars evolve and become supernovae, they destroy their Li. So the newly formed stars would be without Li. Those second-generation stars—main-sequence and turnoff stars—would not have detectable Li. The expectation is that there would be many stars with only upper limits on A(Li). Instead, only in NGC 6752 do a few turnoff stars of the 217 have only upper limits. This issue is highlighted by Shen et al. (2010) in their work about the Li–O anticorrelation in NGC 6752. The polluting gas would have to be enriched in Li. The lack of lithiumless stars among main-sequence and turnoff stars in these globular clusters is one of many unexplained observational puzzles regarding multiple populations in globular clusters. Several anomalies have been discussed in the review by Bastian & Lardo (2018).

Although all of these clusters have similar maximal values of A(Li), that value is lower than the predictions from Big Bang nucleosynthesis. This issue has been discussed by Deal & Martins (2021). That maximum value, about 2.5, could represent a common amount of depletion due rotational effects, as mentioned above. It could also actually be the primordial amount, and the flaw is in some aspect(s) of the predictions.

5. Summary and Conclusions

One method to assess the primordial amount of ^{7}Li is to determine its abundance in the oldest, most unevolved stars. Inasmuch as Li is destroyed in the interiors of stars and diluted at the surfaces of red giants, Li abundances in those evolved stars is not representative of the initial content. The turnoff stars in old and metal-poor globular clusters are plausible subjects for such an investigation. (Main-sequence stars in globular clusters are usually too faint for quality spectral analysis.) In this work we have obtained and analyzed high-resolution spectra of five such stars in the globular cluster M5. These stars are very faint at V = 18.0. With the Keck I telescope and HIRES we obtained and coadded multiple exposures of each of the five stars. The spectral resolution we obtained was ∼45,000 or 0.04 Å pix^{-1}.

We selected stars to be very closely similar to each other. The temperatures of our five stars agree to within 60 K. In spite of that, we found their Li contents range over a factor of 2 with that spread being 5 times the observational error.

We compared these results for M5 with our earlier findings for Li in six turnoff stars in M92 (Boesgaard et al. 1998). Those similar stars showed an even larger array of Li values. The comparisons with results for six clusters were compiled as a function of their metallicities, [Fe/H], in Figure 5. All show a wide range in A(Li), but all have a maximum near A(Li) = 2.5. This is higher than the field star plateau of ∼2.2, but lower than the predicted amount for primordial Li of 2.7–2.8.

The interpretation for the spread in Li values is that the stars had different initial angular momenta and as they spun down, they circulated surface Li down to higher temperatures where it would be destroyed by nuclear reactions with protons, forming 2 He nuclei. The faster rotators would circulate and destroy more Li. It is plausible that all of the stars destroyed some Li from a higher initial amount than the measured 2.5.

If any of the turnoff stars were second- or third-generation cluster members, they would be expected to have no Li. The progenitors would have diluted or destroyed their initial Li. Instead, there are only a few unevolved stars in only one of the six clusters, NGC 6752, with upper limit values for A(Li).

Unevolved stars in these old, very metal-poor globular clusters uniformly show greater amounts of Li than found in the oldest, metal-poor field stars. For each cluster there is a range in Li abundances of at least a factor of 2. The maximum Li amount is the same in all of them at A(Li) ∼2.5. This amount, however, is lower than the predictions from Big Bang nucleosynthesis of 2.7–2.8. It is of interest to extend this study to additional globular clusters.

Acknowledgments

We wish to express our appreciation the Keck Observatory support astronomers for their assistance and knowledge during our observing runs. C.P.D. is grateful for the support through the National Science Foundation grant AST-1909456.

Software: Keck I HIRES Software; IRAF (Tody 1986, 1993); MOOG (Sneden 1973; Sneden et al. 2012).

ORCID iDs

Ann Merchant Boesgaard https://orcid.org/0000-0002-8468-9532
Constantine P. Deliyannis https://orcid.org/0000-0002-3854-050X

References

Aguado, D. S., Gonzalez Herndez, J. I., Allende Prieto, C., et al. 2019, ApJL, 874, L21
Aoki, M., Primas, F., Pasquini, L., et al. 2021, A&A, 653, A13
Bailin, J. 2019, ApJS, 245, 5
Bandyopadhyay, A., Sivarani, T., Beers, T. C., et al. 2022, ApJ, 937, 52
Bastian, N., & Lardo, C. 2018, ARA&A, 56, 83
Boesgaard, A. M. 2004, in Origin and Evolution of the Elements, ed. A. McWilliam & M. Rauch (Cambridge: Cambridge Univ. Press), 117
Boesgaard, A. M., Armengaud, E., King, J. R., Deliyannis, C. P., & Stephens, A. 2004, ApJ, 613, 1202
Boesgaard, A. M., Deliyannis, C. P., & Steinhauer, A. 2005, ApJ, 621, 991
Boesgaard, A. M., Deliyannis, C. P., Stephens, A., & King, J. R. 1998, ApJ, 493, 206
Boesgaard, A. M., Lum, M. G., Chontos, A., & Deliyannis, C. P. 2022, ApJ, 927, 118
Boesgaard, A. M., Lum, M. G., & Deliyannis, C. P. 2020, ApJ, 888, 28
Boesgaard, A. M., Lum, M. G., Deliyannis, C. P., et al. 2016, ApJ, 830, 49
Boesgaard, A. M., & Tripicco, M. J. 1986, ApJL, 302, L49
Bonifacio, P., Pasquini, L., Molaro, P., et al. 2007, A&A, 470, 153
Bonifacio, P., Pasquini, L., Spite, F., et al. 2002, A&A, 390, 91
Carney, B. W. 1983, AJ, 88, 610
Carretta, E., Bragaglia, A., Gratton, R., et al. 2009, A&A, 508, 695
Cayrel, R. 1988, in IAU Symp. 132, The Impact of Very High S/N Spectroscopy on Stellar Physics, ed. G. Cayrel de Strobel & M. Spite (Cambridge: Cambridge Univ. Press), 345
Cyburt, R. H., Fields, D. B., & Olive, K. A. 2008, JCAP, 2008, 12
Cyburt, R. H., Fields, D. B., Olive, K. A., et al. 2016, RvMP, 88, 015004
Deal, M., & Martins, C. J. A. P. 2021, A&A, 653, 48D
Deliyannis, C. P., Anthony-Twarog, B. J., Lee-Brown, D. B., & Twarog, B. A. 2019, AJ, 158, 163
Deliyannis, C. P., Boesgaard, A. M., & King, J. R. 1995, ApJL, 425, L13
Deliyannis, C. P., Boesgaard, A. M., Stephens, A., et al. 1998, ApJ, 498, L147
D'Orazi, V., Angelou, G. C., Gratton, R. G., et al. 2014, ApJ, 791, 39
Endal, A. S., & Sofia, S. 1976, ApJ, 210, 184
Endal, A. S., & Sofia, S. 1981, ApJ, 243, 625
Gonzalez Hernandez, J. L., Bonifacio, P., Caffau, E., et al. 2009, A&A, 505, L13
Gratton, R. G., Carretta, E., & Bragaglia, A. 2012, A&ARv, 20, 50
Gruyters, P., Nordlander, T., & Korn, A. J. 2014, A&A, 567, A72
Jeffries, R. D., Jackson, R. J., Sun, Q., & Deliyannis, C. P. 2021, MNRAS, 500, 1158
King, J. R. 1993, AJ, 106, 1206
Koch, A., Lind, K., & Rich, R. M. 2011, ApJL, 738, L29
Lardo, C., Salaris, M., Cassini, S., et al. 2023, A&A, 669, A19
Lind, K., Primas, F., Charbonnel, C., et al. 2009, A&A, 503, 545
Monaco, L., Villanova, S., Bonifacio, P., et al. 2012, A&A, 539, A157
Pasquini, L., Bonifacio, P., Molaro, P., et al. 2005, A&A, 441, 549
Pasquini, L., & Molaro, P. 1996, A&A, 307, 761
Pasquini, L., & Molaro, P. 1997, A&A, 322, 109
Pinsonneault, M. H., Deliyannis, C. P., & Demarque, P. 1992, ApJS, 78, 179
Pinsonneault, M. H., Kawaler, S. D., Sofia, S., & Demarque, P. 1989, ApJ, 338, 424
Ramirez, I., & Melendez, J. 2005, ApJ, 626, 465
Ryan, S. G., & Deliyannis, C. P. 1995, ApJ, 453, 819
Sandquist, E. L., Bolte, M., Stetson, P. B., et al. 1996, ApJ, 470, 910
Schiappacasse-Ulloa, J., Lucatello, S., Rain, M. J., et al. 2022, MNRAS, 511, 231
Shen, Z.-X., Bonifacio, P., Pasquini, L., et al. 2010, A&A, 524, L2
Sills, A., & Deliyannis, C. P. 2000, ApJ, 544, 944
Sneden, C. 1973, ApJ, 184, 839
Sneden, C., Bean, J., Ivans, I., et al. 2012, MOOG: LTE Line Analysis And Spectrum Synthesis, Astrophysics Source Code Library, asc1:1202.009
Sneden, C., Kraft, R. P., Prosser, C. F., et al. 1992, AJ, 104, 2121
Somers, G., & Pinsonneault, M. H. 2015, MNRAS, 449, 4131
Somers, G., & Pinsonneault, M. H. 2016, ApJ, 829, 32
Spite, F., & Spite, M. 1982, A&A, 115, 357
Spite, M., Spite, F., Gallagher, A. J., et al. 2016, A&A, 594, A79
Sun, Q., Deliyannis, C. P., Steinhauer, A., et al. 2023, ApJ, 952, 71
Thorburn, J. A., Hobbs, L. M., Deliyannis, C. P., & Pinsonneault, M. H. 1993, ApJ, 415, 150
Tody, D. 1986, Proc. SPIE, 627, 733
Tody, D. 1993, in ASP Conf. Ser. 52 Astronomical Data Analysis Software and Systems II, ed. R. J. Hanisch et al. (San Fransisco CA: ASP), 173
Valcin, D., Bernal, J. L., Jimenez, R., et al. 2020, JCAP, 2020, 002
Vogt, S. S., Allen, S. L., Bigelow, B. C., et al. 1994, Proc. SPIE, 2198, 362
Wang, E. X., Norlander, T., Asplund, M., et al. 2021, MNRAS, 500, 2159
Ying, J., Chaboyer, B., & Boudreaux, E. M. 2023, AJ, 166, 18
Zinn, R., & West, M. J. 1984, ApJS, 55, 45